



# Titration of chiral kink sites on Cu(643) using iodine adsorption

Preeti Kamakoti <sup>a,b</sup>, Joshua Horvath <sup>a</sup>, Andrew J. Gellman <sup>a</sup>, David S. Sholl <sup>a,b,\*</sup>

<sup>a</sup> Department of Chemical Engineering, Carnegie Mellon University, Pittsburgh, PA 15213, USA

<sup>b</sup> National Energy Technology Laboratory, Pittsburgh, PA 15236, USA

Received 19 February 2004; accepted for publication 14 June 2004

Available online 25 June 2004

## Abstract

Density functional theory (DFT) and temperature programmed desorption (TPD) experiments have been used to probe the site preferences of adsorbed iodine atoms on Cu surfaces. DFT calculations are presented for iodine adsorption on Cu(111), Cu(100), Cu(221), Cu(533), Cu(531), and Cu(643). Additional DFT calculations are presented for I adsorption on a stepped Cu surface that mimics a thermally roughened Cu(643) surface. The molecular desorption of R-3-methylcyclohexanone from clean and iodine precovered Cu(643) has been used to experimentally examine the location of iodine on this surface. Our results show that there is a strong energetic preference for iodine to adsorb at step edges on Cu surfaces vicinal to Cu(111) and that when kinks are present in surface steps, iodine prefers to adsorb in the vicinity of these kinks over adsorbing along straight step edges. Thus, the adsorption of atomic iodine can be used to selectively titrate the kink sites on intrinsically chiral Cu surfaces vicinal to Cu(111).

© 2004 Elsevier B.V. All rights reserved.

**Keywords:** Stepped single crystal surfaces; Copper; Iodine; Density functional calculations; Thermal desorption spectroscopy

## 1. Introduction

The observation that high Miller index surfaces of metals are intrinsically chiral has led to a number of efforts to use these chiral environments for enantiospecific adsorption and chemistry [1–5]. High Miller index surfaces are characterized by atomically flat terraces separated by kinked steps. Providing a detailed description of molecular adsorption on these surfaces is complicated by the

existence of many structurally distinct binding sites [4–6]. Among this collection of binding sites, it is particularly important to be able to distinguish between sites associated with locally achiral regions of the surface, that is, terraces and straight step edges, and the locally chiral regions associated with kinks in surface steps. In this paper, we use a combination of density functional theory (DFT) calculations and temperature programmed desorption (TPD) experiments to show that the adsorption of atomic iodine on chiral Cu surfaces vicinal to Cu(111) can be used to selectively titrate the chiral binding sites associated with kinked steps on these surfaces.

\* Corresponding author. Tel.: +1-412-268-4207; fax: +1-412-268-7139.

E-mail address: [sholl@andrew.cmu.edu](mailto:sholl@andrew.cmu.edu) (D.S. Sholl).

The adsorption of atomic iodine on Cu(111) and Cu(100) has been studied in a number of previous experiments [7–14]. We discuss the details of these previous studies below by comparing the results of our DFT calculations with the experimental observations. In general terms, one of the main conclusions from these studies is that I atoms adsorb in the most highly coordinated sites on these two flat surfaces, namely, the three-fold and four-fold sites on Cu(111) and Cu(100), respectively. If this preference for highly coordinated sites also applies to stepped surfaces, it may be expected that I atoms will preferentially bind below step edges. We will show below that while iodine does indeed prefer to bind near surface steps, it does not do so in a way that maximizes its coordination with surface atoms.

The paper is organized as follows. In Section 2, our theoretical and experimental methods are described. Section 3 describes our DFT results for I adsorption on flat Cu surfaces and compares our results with available experimental data. Our DFT calculations examining the adsorption of I on stepped and kinked Cu surfaces vicinal to Cu(111) are presented in Section 4, and our experimental results probing the siting of I on Cu(643) are described in Section 5. We conclude in Section 6 with a discussion of the identity of desorption products that occur when I desorbs from Cu surfaces at high temperatures.

## 2. Methods

### 2.1. Theoretical

We investigated the adsorption of atomic I on a number of Cu surfaces using density functional theory. All calculations were performed using the Vienna ab-initio simulation package (VASP) [15]. These calculations examine material of infinite extent by using supercells with periodic boundary conditions in all three principal directions. Electron exchange correlation effects were described via the generalized gradient approximation (GGA) using the Perdew–Wang 91 functional. A plane wave expansion with a cutoff of 233.7 eV was used in all calculations. The geometry was relaxed using a

quasi-Newton algorithm until the forces on all unconstrained atoms were less than 0.03 eV/Å. A Monkhorst–Pack mesh with a  $5 \times 5 \times 1$   $k$ -grid was used for Cu(111), Cu(100), and Cu(531) surfaces. A  $6 \times 6 \times 1$   $k$ -grid was used for the stepped Cu(221), Cu(533) and Cu(643) and thermally roughened non-Miller index Cu(643) surfaces. A supercell consisting of four Cu layers was used in calculations on atomically flat surfaces. Atoms in the top two Cu layers and the I adlayer were allowed to completely relax in all directions, while the remaining two layers were fixed at their bulk equilibrium positions with the lattice spacing determined by DFT. For all other surfaces, the supercell consisted of layers that had a thickness equivalent to three layers of the Cu(111) supercell. In these cases, Cu atoms equivalent in thickness to a single (111) layer and the I adlayer were allowed to relax completely. A vacuum spacing equivalent to 4–5 lattice spacings was used in all calculations. The lattice constant and bulk modulus for Cu optimized using the GGA were found to be 3.64 Å and 152 GPa, in good agreement with experimental values of 3.61 Å and 142 GPa, respectively [16].

Adsorption energies were defined based on the following expression for the dissociative adsorption of molecular iodine,

$$E_{\text{ads}} = \left[ E_{\text{Cu}} + \frac{1}{2} E_{\text{I}_2} - E_{\text{I,ads}} \right], \quad (1)$$

where the terms on the right are the total energy of the bare Cu surface, gaseous  $\text{I}_2$ , and of the Cu surface with an I adlayer, respectively. With this definition, more positive values of  $E_{\text{ads}}$  indicate stronger binding of I to the surface. On stepped surfaces, we describe the height of I adatoms by the perpendicular distance of the adatom above the plane defined by the surface atoms in the terrace forming the upper portion of the step. We used the following labeling convention for adsorption sites on stepped and kinked surfaces. Sites along A type step edges formed by (100) microfacets, B type step edges formed by (110) microfacets and on terraces were denoted as A, B, and T, respectively, with an additional numeric subscript  $n$  (e.g.  $A_n$ ) to differentiate multiple sites. Kink and corner sites were labeled as K and C, respectively.

## 2.2. Experimental

The site preferences for adsorbed I were examined experimentally by performing temperature programmed desorption (TPD) studies of R-3-methylcyclohexanone (R-3-MCHO) from Cu(643) single crystal surfaces in ultra-high vacuum. We have shown previously that R-3-MCHO desorbs molecularly from Cu surfaces and that the observed desorption spectrum from Cu(643) exhibits three distinct sub-monolayer peaks at 230, 345, and 385 K that can be unambiguously attributed to desorption from terrace, straight step edge, and kink features, respectively [3,17].

Atomic iodine was deposited onto the Cu(643) and Cu(111) surfaces by adsorbing iodoethane onto a clean surface at approximately 100 K. Subsequent heating causes cleavage of the C–I bond in the adsorbed iodoethane producing adsorbed atomic I and ethyl groups. This is followed by  $\beta$ -hydride elimination of the ethyl groups and finally, desorption of ethylene at temperatures below 300 K [12,13]. Since atomic I is stable on Cu surfaces up to temperatures of roughly 900 K, this process leaves atomic I on the surface. The maximum iodine coverage attainable using this procedure is limited by the competition between adsorbed I and ethyl groups [14]. Higher total iodine coverages were achieved by repeated cycles of first exposing the surface to 2 L (or less) of iodoethane and then heating to 300 K. The cumulative ethylene desorbed from a Cu(111) surface following each cycle is shown (for several independent experiments) in Fig. 1. Since ethylene and iodine are initially present on the surface in equimolar quantities, the cumulative ethylene desorption accurately assesses the total iodine coverage on the surface. It can be seen from Fig. 1 that cumulative iodoethane exposures of approximately 10 L were required to saturate the Cu(111) surface with I. This saturated surface yielded a sharp low energy electron diffraction (LEED) pattern consistent with a  $(\sqrt{3} \times \sqrt{3})R30^\circ$  I adlayer [9]. Similar cumulative exposures of iodoethane were found to saturate the I coverage on Cu(643), although no ordered LEED pattern was observed from the I adlayer.

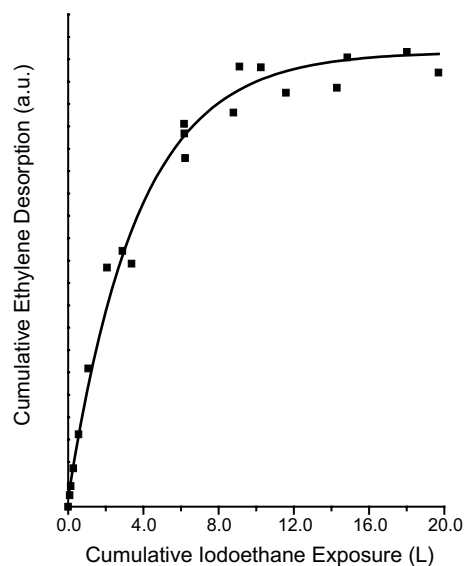


Fig. 1. Cumulative desorption of ethylene observed from Cu(111) following repeated cycles of exposure to 2 L or less of iodoethane at 100 K and heating to 300 K.

The desorption of R-3-MCHO from iodine precovered Cu(643)<sup>R</sup> surfaces was studied by first depositing an I adlayer on an initially clean surface following the method described above. The R designation of this surface stems from the fact that it is an intrinsically chiral surface [3]. This designation is only included for completeness; all of the conclusions drawn below also apply to Cu(643)<sup>S</sup>. The surface was then cooled to 100 K and exposed to 0.01 L of R-3-MCHO introduced into the UHV chamber through a doser. The capillary array doser creates an enhancement in pressure at the sample surface over that measured in the chamber background. Using the doser, a 0.01 L exposure is sufficient to create a monolayer of R-3-MCHO on the surface in the absence of any adsorbed atomic I [3]. TPD spectra of R-3-MCHO were then collected by heating at 1 K/s while monitoring the mass spectrometry signal at  $m/q = 37$ . The same sputtering and annealing procedure used in our earlier experiments with Cu(643) [2,3,18] was sufficient to remove the iodine from the Cu surface at the conclusion of an experiment. To ensure that all experiments were performed with the equivalent initial surface conditions, the surface was sputtered and annealed between experiments and a

new layer of iodine was applied to the surface before each desorption experiment.

### 3. Iodine adsorption on Cu(111) and Cu(100)

LEED [8,9] and STM studies [10] have reported the formation of a  $(\sqrt{3} \times \sqrt{3})R30^\circ$  adlayer of I on Cu(111) at a coverage of 0.33 ML when the surface is saturated by exposure to gaseous  $I_2$ . A SEXAFS study [7] determined that the three-fold hollow site is the favored adsorption site with a Cu–I bond length of  $2.66 \pm 0.02$  Å. The same SEXAFS study examined a  $p(2 \times 2)$  adlayer with a coverage of 0.25 ML on Cu(100), yielding a Cu–I bond length of  $2.69 \pm 0.02$  Å. The binding site on the Cu(100) surface is the four-fold hollow. On both surfaces the preferred binding site is the high coordination site.

We used DFT calculations to examine the adsorption of I as a  $(\sqrt{3} \times \sqrt{3})R30^\circ$  adlayer on Cu(111). All four high symmetry adsorption sites on the surface, fcc three-fold, hcp three-fold, bridge, and top, were considered as potential adsorption geometries. The resulting adsorption energies and geometries are summarized in Table 1. Consistent with the experimental observation listed above, I adsorbs most favorably in the three-fold hollow sites. There is no detectable energy difference between adsorption at the fcc and hcp sites in our calculations, and the resulting Cu–I bond lengths, 2.68 Å, are in excellent agreement with the experimental result,  $2.66 \pm 0.02$  Å [7]. This bond length is different from that of the gas phase Cu–I halide, an observation that supports structural and photoemission studies that indicate the chemisorbed state is distinct from the metal halide [11]. The bridge site is found to be the transition

Table 1

Adsorption energies and Cu–I bond lengths for a  $(\sqrt{3} \times \sqrt{3})R30^\circ$  I adlayer on Cu(111) with a coverage of 0.33 ML

Adsorption site	Energy (eV)	Bond length (Å)
fcc	1.44	2.68
hcp	1.44	2.68
Bridge	1.40	2.60
Top	1.14	2.49

Table 2

Adsorption energies and Cu–I bond lengths for a  $p(2 \times 2)$  I adlayer on Cu(100) with a coverage of 0.25 ML

Adsorption site	Energy (eV)	Bond length (Å)
Hollow	1.67	2.75
Bridge	1.49	2.59
Top	1.21	2.50

state for diffusion between adjacent fcc and hcp sites. It is interesting to note that the activation energy for I diffusion on Cu(111) predicted by these calculations, 0.04 eV, is small. To estimate the adsorption energy of an isolated I atom, we performed calculations on an I adlayer having a coverage of 0.11 ML corresponding to an I density of one adatom per  $14.2$  Å<sup>2</sup> [2]. This calculation yielded an adsorption energy of 1.62 eV, nearly 0.2 eV larger than the adsorption energy for the  $(\sqrt{3} \times \sqrt{3})R30^\circ$  adlayer. This comparison suggests that island formation by adsorbed iodine is not favored at low coverages.

We performed analogous DFT calculations for a  $p(2 \times 2)$  adlayer of I on Cu(100), again examining each of the surface's high symmetry sites as potential adsorption sites. The resulting binding energies and Cu–I bond lengths are summarized in Table 2. The four-fold hollow site is clearly the favored adsorption site with a binding energy of 1.67 eV. The bond length observed for this site, 2.75 Å, is in good agreement with the SEXAFS result of  $2.69 \pm 0.02$  Å [7]. Similarly to Cu(111), the bridge site is found to be a transition state for I diffusion. The diffusion activation energy predicted by our calculations on Cu(100), 0.18 eV, is considerably larger than the analogous quantity on Cu(111). As on the (111) surface, we examined the adsorption energy of an isolated I adatom by considering an I adlayer with a coverage of 0.11 ML. This calculation yields a binding energy of 1.80 eV.

## 4. DFT results for I adsorption on stepped Cu surfaces

### 4.1. I adsorption on Cu(221) and Cu(533)

DFT calculations were performed for Cu(221) and Cu(533), two Cu surfaces with straight steps

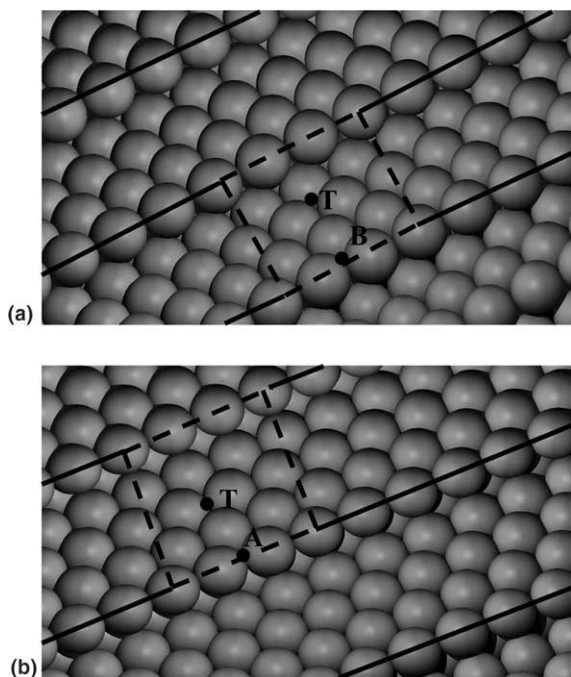


Fig. 2. Illustrations of (a) Cu(221) and (b) Cu(533). In each case, the solid line indicates the step edge and the adsorption sites described in Table 3 are marked.

that separate (111) oriented terraces. These surfaces are illustrated in Fig. 2. The step edges on these two surfaces differ in their local orientation; on Cu(221) the step edge is a (110) microfacet, while the step edge on Cu(533) is a (100) microfacet [4]. Calculations were performed with I densities of one adatom per  $15.4 \text{ \AA}^2$  on Cu(221) and  $17.9 \text{ \AA}^2$  on Cu(533). These densities are equivalent to coverages of 0.10 and 0.09 ML, respectively, on Cu(111). On both surfaces, the unit cells were three atoms wide along the step edge and spanned the terrace between adjacent steps, as shown in Fig. 2. Adsorption energies were computed at several adsorption sites along the step edge and a three-fold site in the center of each surface's terrace. The resulting binding energies for the most stable site along the step edge and for the terrace site are listed in Table 3. The two surfaces yield very similar results; both exhibit adsorption energies of approximately 1.4 eV on their terraces and considerably stronger binding energies of approximately 1.7 eV at the step edge. In the case

Table 3

Adsorption energies for I at step (A) and terrace (T) sites on Cu(221) and Cu(533) corresponding to coverages of 0.10 and 0.09 ML, respectively

Adsorption site	Cu(221) B	Cu(221) T	Cu(533) A	Cu(533) T
Energy (eV)	1.69	1.39	1.69	1.42

of I on Cu(221), its preferred binding site is at the three-fold hollow site above the step edge. At this site, the Cu–I bond length with its three nearest neighbor atoms around the step edge is  $2.50 \text{ \AA}$  and the adsorbed atom lies  $1.94 \text{ \AA}$  vertically above the plane defined by the upper terrace. I adsorption on Cu(533) takes place at the top of the step edge, where the adsorbed atom is located above an edge-bridge site. The Cu–I bond length with the two atoms on the edge bridge site was  $2.48 \text{ \AA}$ , and the I atom was located at a height of  $2.02 \text{ \AA}$  above the plane defining the upper terrace.

Our observations for atomic I adsorption are qualitatively similar to previous studies of other electronegative atoms adsorbing on steps of metal surfaces. A combined first principles and STM study examined the binding sites of electronegative oxygen on stepped Pt(111) surfaces [19]. For the (100) step edge, O was found to adsorb preferentially at the edge bridge site rather than the adjacent three-fold site on the upper (111) microfacet. O atoms favored the three-fold hollow site adjacent to the step edge on Pt surfaces with (110) step edges. Similar results were found for the adsorption of S on Al(331), which has (100) steps [20].

#### 4.2. I adsorption on Cu(531) and Cu(643)

The fact that single crystal surfaces of metals with kinked step edges are inherently chiral has led to a great deal of interest in the properties of such surfaces [2,4,5,21]. To examine the adsorption of I on surfaces with kinked step edges, we first performed calculations for the ideal termination of Cu(531), which has the smallest unit cell among all such chiral surfaces [1,4]. This surface is illustrated in Fig. 3. Placing one I atom per unit cell on this surface results in an adlayer density of one atom per  $5.4 \text{ \AA}^2$ , equivalent to a coverage of 0.29

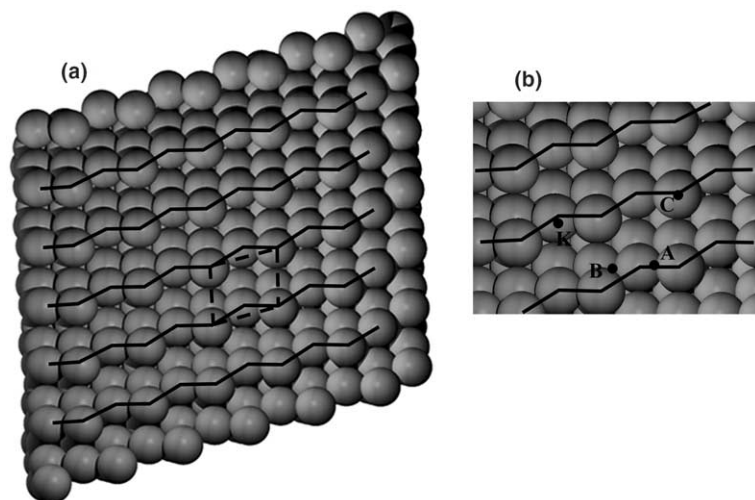


Fig. 3. (a) A view of the Cu(531) surface with the step edges and surface unit cell denoted by solid lines and dashed lines, respectively. (b) Another view of the Cu(531) surface with the adsorption sites listed in Table 4 marked.

ML on Cu(111). Using results from our calculations on flat and stepped surfaces as a guide, 13 potential adsorption sites were examined. In several cases, the adsorbed I moved significantly from its initial position during structural relaxation. The four distinct minima that were found from these 13 calculations are labeled on Fig. 3(b) and listed with their binding energies in Table 4. The strongest adsorption site (site K) was found to be in the kink region, while adsorption on top of the corner atom (site C) was found to be energetically unfavorable. At site A, the adsorbed I lies  $\sim 1.65$  Å vertically above the region defining the upper (111) microfacet. The Cu–I bond length with the nearest neighbor Cu atom at the kink was 2.59 Å. Site B, corresponding to adsorption at a three-fold site above the (110) microfacet, was only slightly less energetically favored than site K. In contrast, adsorption at the three-fold site above the (100)

microfacet (site C) was  $\sim 0.1$  eV less stable than at the kink (site K).

We have examined I adsorption in a similar fashion on Cu(643), a kinked stepped surface illustrated in Fig. 4. The ideal termination of Cu(643) has (111) terraces separated by a step edge that alternates between segments of (110)-oriented kinks and (100)-oriented steps that are two atoms in length [2,4,21]. Placing one I atom per unit cell on this surface results in an adlayer with a density of one I per  $14.2$  Å<sup>2</sup>, equivalent to a 0.11 ML coverage on Cu(111). As on Cu(531), a range of initial positions were used to determine local minima for I adsorption on Cu(643). Only one of these initial positions was chosen to represent a three-fold site on the terrace; the others were used to examine possible adsorption sites associated with the step edge. The positions of the four local adsorption minima found in this way are illustrated in Fig. 4(b), and the binding energies at these sites are listed in Table 5. As with the straight stepped surfaces examined above, there is a significant energetic preference for I atoms to adsorb near the step edge (sites B, A<sub>1</sub>, and A<sub>2</sub>) rather than on the terrace (site T). In its most favored binding position (site A<sub>2</sub>), I is adsorbed at a bridge site on the (100) step edge, roughly one atom away from the kink. In this site, the adsorbed I atom lies 3.75

Table 4  
Adsorption energies for I binding sites on Cu(531) with a coverage of 0.29 ML

Adsorption site	K	B	A	C
Energy (eV)	1.75	1.72	1.66	-0.71

Labels for the sites correspond to the labels shown in Fig. 3(b).

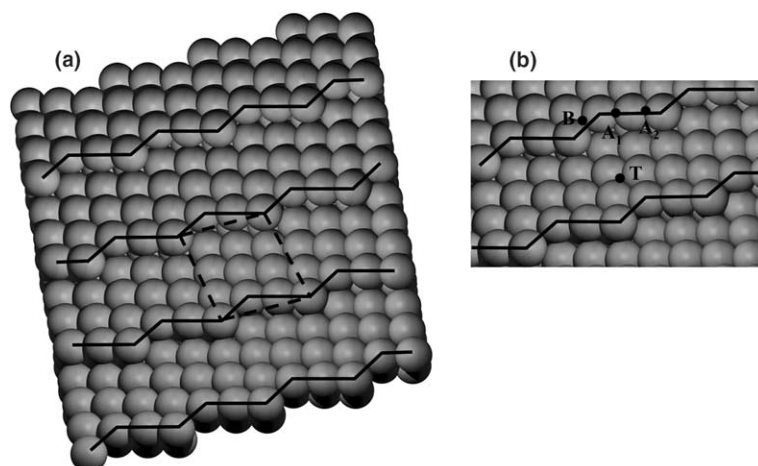


Fig. 4. (a) A view of the Cu(643) surface with the step edges and surface unit cell denoted by solid lines and dashed lines, respectively. (b) Another view of the Cu(643) surface with the adsorption sites listed in Table 5 marked.

Table 5

Adsorption energies for I binding sites on Cu(643) with a coverage of 0.11 ML

Adsorption site	B	A <sub>1</sub>	A <sub>2</sub>	T
Energy (eV)	1.66	1.71	1.73	1.54

Labels for the sites correspond to the labels shown in Fig. 4(b).

Å away from the kink atom and 2.08 Å vertically above the upper (111) terrace. The Cu–I bond lengths with the two Cu atoms forming the step edge were 2.58 and 2.54 Å. Site A<sub>1</sub>, corresponding to adsorption at the kink above the (100) step, is ~0.04 eV less stable than the most favored site. The I atom is displaced 1.54 Å away from the kink atom and 2.11 Å vertically above the upper terrace. The bond lengths with the atoms on the edge bridge were 2.80 and 2.61 Å. Adsorption on top of the (110) step edge (site B) was ~0.07 eV less favorable than at site A<sub>2</sub>. In this position, the I atom is located 1.29 Å away from the kink and 2.37 Å vertically above the terrace. The bond lengths as defined above for the other sites were 2.54 and 2.64 Å.

#### 4.3. Adsorption on thermally roughened Cu(643)

The results above have examined the adsorption of iodine on the ideal terminations of Cu(531) and Cu(643). Real stepped metal sur-

faces often differ markedly from their ideal terminations due to disorder induced by thermal fluctuations in the positions of the step edges, that is, thermal roughening [4,6,22–24]. STM experiments examining stepped Cu surface vicinal to Cu(100) [25] and Cu(111) [26] have shown that while these surfaces typically retain their monoatomic steps, the local structure of their steps can be subject to strong fluctuations. In addition to broadening the distributions of step lengths and terrace widths that exist on a surface, thermal fluctuations can create local environments that cannot exist on perfect Miller index surfaces. For example, real stepped surfaces can have kink sites formed by the intersection of two straight step edges that are both more than one atom long. In contrast, on perfect Miller index surfaces, one of the two step edges that forms a kink site must be just one atom long [4,6,24] (see, for example, Figs. 3 and 4). Theoretical studies of molecular adsorption on stepped Pt surfaces with realistic thermally equilibrated structures have suggested that, at least in some instances, adsorption at the so-called non-Miller index kinks can dominate the low coverage behavior of real surfaces [6].

To probe the adsorption of I on thermally roughened kinked stepped Cu surfaces, we performed DFT calculations using a Cu surface created to include a non-Miller index kink. This

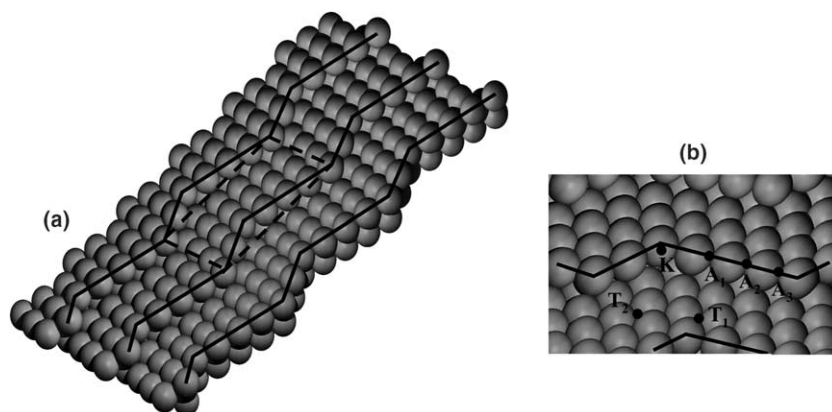


Fig. 5. Two views of the hypothetical non-Miller index surface obtained by modifying the Cu(643) surface as discussed in the text. The adsorption sites marked in (b) correspond to those listed in Table 6.

surface, which is shown in Fig. 5, was created by using a supercell containing two Cu(643) supercells in the direction parallel to the step edge. The step edge atoms were then rearranged to give a step edge that was two and four atoms long along the (110) and (100)-step edges, respectively. Placing one I atom in this supercell corresponded to a density of one adatom per  $28.4 \text{ \AA}^2$  or a coverage of 0.05 ML with respect to Cu(111). A series of adsorption sites along the step edges and two terrace sites were studied. These sites and the resulting binding energies are shown in Fig. 5 and Table 6, respectively. Site K, corresponding to adsorption at the kink, was found to be the most energetically favored site. In this site, the I atom is  $2.02 \text{ \AA}$  above the plane defined by the upper terrace. The Cu–I bond length formed with its nearest neighbor kink atom is  $2.49 \text{ \AA}$ . When I adsorbs at site  $A_1$ , an edge bridge site on the (100) step edge, the binding energy is  $\sim 0.05 \text{ eV}$  lower than site K. Adsorption at sites  $A_2$  and  $A_3$ , which are also on

the (100) step edge but are more distant from the kink site, are  $0.13 \text{ eV}$  less stable than the kink site. Similar to the other stepped surfaces that we examined, the terrace sites on this surface have considerably lower binding energies than the adsorption sites located along the step edges.

The binding energies calculated for I at terrace sites on the stepped surfaces we have examined are not identical to those calculated on Cu(111). For example, the three-fold terrace site that we examined on Cu(643) gave a binding energy of  $1.54 \text{ eV}$  (see Table 5). At the equivalent surface coverage on Cu(111), we calculated a binding energy of  $1.62 \text{ eV}$ . These variations occur at least in part because of different adatom–adatom interactions among the different unit cell geometries. The results from our non-Miller index surface are therefore particularly important, because they unambiguously demonstrate the significant energy difference ( $>0.3 \text{ eV}$ ) between terrace sites and step edge sites in a series of completely self-consistent calculations for surfaces with relatively wide terraces.

Table 6

Adsorption energies for I binding sites on a hypothetical non-Miller index surface obtained by modifying the Cu(643) surface with a coverage of 0.05 ML

Adsorption site	K	$A_1$	$A_2$	$A_3$	$T_1$	$T_2$
Energy (eV)	1.80	1.75	1.68	1.67	1.50	1.43

Labels for the sites correspond to the labels shown in Fig. 5(b).

## 5. Experimental results for I adsorption on Cu(643)

TPD spectra observed for the desorption of R-3-MCHO from clean and I precovered Cu(643) are shown in Fig. 6. The spectrum drawn with the thick line corresponds to desorption of

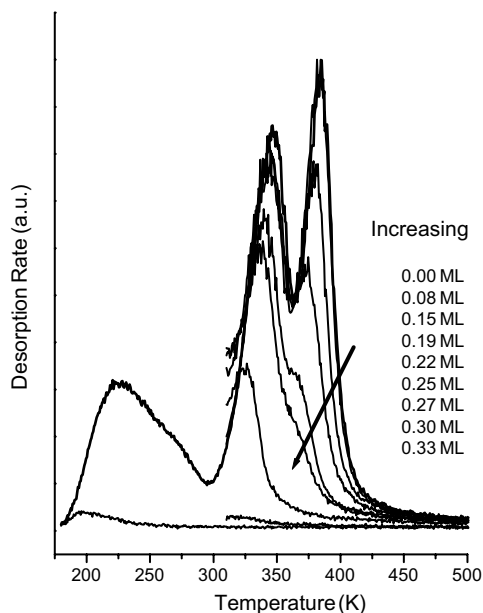


Fig. 6. Temperature programmed desorption spectra of R-3-MCHO from I modified Cu(643). The thick curve is the TPD spectrum from the clean Cu(643) surface. The thin curves are TPD spectra of R-3-MCHO from Cu(643) surfaces with different preadsorbed coverages of I atoms. In each experiment with the I precovered surface, an exposure of R-3-MCHO sufficient to create a monolayer of R-3-MCHO on clean Cu(643) was used.

R-3-MCHO from clean Cu(643), which has been discussed in detail elsewhere [3]. This spectrum shows three distinct peaks at 230, 345, and 385 K. Comparison with analogous TPD spectra on Cu(111) indicate that the peak at 230 K can be assigned to molecules desorbing from (111) terraces. Comparison with desorption spectra obtained from Cu surfaces with straight steps makes it clear that peak at 345 K in Fig. 6 can be associated with molecules desorbing from straight step edges [3,17]. The implication is that the desorption peak at 385 K on the clean Cu(643) surface must arise from molecules desorbing from the kinks. In interpreting these spectra, it is important to note that the real structure of Cu(643) surfaces is significantly more disordered than the ideal termination shown in Fig. 4 because of thermal disorder in the step edges, as discussed above. Detailed models of thermal disorder for similar Pt surfaces [6,24] and STM images of stepped Cu surfaces

[25,26] have shown that in general, the steps of real high index surfaces have fewer kinks and longer straight step edges than exist on ideal surface terminations. For similar reasons, the number of terrace sites available for adsorption is larger on real high Miller index surfaces than on ideally terminated high Miller index surfaces.

The spectra drawn with the narrow lines in Fig. 6 have been obtained from surfaces modified by the initial adsorption of increasing amounts of atomic I followed by exposures to R-3-MCHO sufficient to adsorb one monolayer on the clean surface. To avoid confusion and highlight the effects of adsorbed I on R-3-MCHO desorption from the step and kink sites, the TPD spectra in the temperature regime below 315 K have not been shown. It is clear from Fig. 6 that the adsorption of I on Cu(643) reduces the intensity of the peaks associated with R-3-MCHO desorption from kinked and straight step edges. When the surface is precovered with 0.33 ML of I, as calibrated using Fig. 1, no desorption of R-3-MCHO is observed in the temperature range shown in Fig. 6. As the I coverage is increased from zero, the highest temperature peak in the TPD spectra disappears first, followed by the subsequent disappearance of the lower temperature peak. It is evident from these results that I atoms block the adsorption of R-3-MCHO. More importantly, these experiments show that at low coverages, I preferentially blocks adsorption of R-3-MCHO at kink sites. Thus, these experiments strongly indicate that I atoms preferentially adsorb close to kinks on Cu(643). This observed trend supports the DFT calculations reported above.

## 6. Discussion

We have used a combination of DFT calculations and TPD experiments to examine the site preferences for atomic I on flat and stepped Cu surfaces. Our DFT results for Cu(100) and Cu(111) give binding geometries in quantitative agreement with earlier experimental measurements for these quantities. On these flat surfaces, I binds in the surface site that maximizes its coordination with the underlying metal atoms. Our DFT cal-

culations for a range of Cu surfaces vicinal to Cu(111) indicate that the binding energies of I atom adsorption at sites along step edges are significantly stronger than those for adsorption sites on surface terraces. Step edge sites do not, however, necessarily maximize the coordination of I atoms with the surface; in most cases I is found to be positioned well above the step edge. By examining a non-Miller index surface that exhibits both kinks and long straight step edges, we are able to conclude that the binding of I at sites near kinks is significantly favored over binding at straight step edges, although both these types of sites are favored over terrace sites. We have further examined this general picture by examining the molecular desorption of 3-MCHO from I precovered Cu(643). In its thermally equilibrated state, Cu(643) exhibits both straight step and kink sites, in addition to its (111) terraces. Our experiments show that adsorbing small amounts of I preferentially blocks 3-MCHO adsorption at kink sites and that increasing the coverage of I subsequently blocks molecular adsorption at straight step sites. Thus, our theoretical and experimental results provide a consistent description of the site preferences for I adsorption on stepped Cu surface vicinal to Cu(111). Of particular importance for efforts to understand the properties of chiral molecules on intrinsically chiral metal surfaces, our results show that adsorption of atomic I can selectively titrate the binding sites associated with the locally chiral kinks of chiral Cu surfaces vicinal to Cu(111).

Our discussion throughout this paper has focused on the adsorption of I on Cu surfaces that are viewed as static objects. It is of course possible for the adsorption of atomic or molecular species to lead to restructuring of surfaces by changing the free energies associated with various surface configurations. The energetic preference for I to adsorb at kink sites over straight step sites may have interesting implications for the thermally equilibrated structures of Cu surfaces with nominally straight step edges in the presence of small quantities of adsorbed iodine. In these cases, the adsorbed I is likely to stabilize kinks that are formed by thermal fluctuations, thereby increasing the equilibrium kink density of the resulting step

edges. An additional possibility is that I would effectively etch surface steps via the formation of a copper iodide layer (as distinct from the chemisorption of atomic I that we have considered). Our DFT calculations provide little insight into this possibility; we can only make the unsurprising statement that if this process occurs then it must involve an activation barrier. A slightly stronger conclusion can be drawn from our experiments. Low coverages of surface I do not strongly disrupt the multi-peak structure observed in TPD of R-3-MCHO from the bare surface (see Fig. 6). This observation suggests that the perturbation of the bare surface step structure due to adsorbed I is not great.

While our focus in this paper has mainly been on the site preferences for adsorbed I on Cu surfaces, we can also use our results to discuss the desorption products that result from heating iodine covered Cu surfaces. Experimental work by Jenks et al. [12,13] reported desorption of CuI and Cu sublimation. This and a TPD study [27] reported peak desorption temperatures of 900–950 K, corresponding to an energy barrier of  $\sim 2.5$  eV assuming a first-order desorption process. We estimated the energies for desorption of atomic I, I<sub>2</sub>, and CuI from the  $(\sqrt{3} \times \sqrt{3})R30^\circ$  adlayer on Cu(111) from our DFT calculations using

$$E_{\text{des}} = E_{\text{Cu}} + E_{\text{prod}} - E_{\text{I,ads}}, \quad (2)$$

where the terms on the right are the total energy of the final surface after desorption, the gaseous final product, and the original metal surface with an I adlayer. For desorption of I<sub>2</sub>, Eq. (2) was applied based on an area of the surface initially containing two I atoms. In all cases, use of Eq. (2) assumes that there are no additional barriers to desorption other than the energy required to move the desorbing species from the surface into the gas phase. Under these assumptions, Eq. (2) yields desorption energies of 2.55, 2.88, and 3.83 eV for I, I<sub>2</sub>, and CuI from the  $(\sqrt{3} \times \sqrt{3})R30^\circ$  adlayer on Cu(111). Thus, our calculations indicate that desorption of atomic I is strongly preferred over the desorption of CuI. To probe the origin of the experimentally observed desorption of CuI, we performed a series of DFT calculations examining Cu sublimation from Cu atoms with a range of coordinations. Our

calculated sublimation energies varied from approximately 2.0 eV for a Cu atom in a three-fold site on a (1 1 1) surface to 4.2 eV for a nine-fold coordinated Cu atom from the top layer of a (1 1 1) surface. Moreover, we find that the desorption energy for CuI from a given surface atom is always less than that for the Cu atom alone. Thus, there are a large number of desorption pathways for Cu and for CuI from defect sites on nominally (1 1 1) surfaces that have desorption energies similar to or less than those for atomic I desorption from the  $(\sqrt{3} \times \sqrt{3})R30^\circ$  adlayer. Since it is likely that there are many surface defects at the elevated temperatures associated with these desorption products, our results support the idea that a range of desorption products may be observed with a strong contribution to these products arising from surface defects [11]. If under any experimental conditions, surface iodine can form a copper iodide layer on part or all of a surface, then this layer could also contribute to the observation of CuI desorption when these surfaces are heated to high temperatures.

### Acknowledgements

This work was partially supported by the NSF (CTS-0216170). DSS is an Alfred P. Sloan fellow.

### References

- [1] G.A. Attard, *J. Phys. Chem. B* 105 (2001) 3158.
- [2] A.J. Gellman, J. Horvath, *J. Am. Chem. Soc.* 123 (2001) 7953.
- [3] J.D. Horvath, A.J. Gellman, *J. Am. Chem. Soc.* 124 (2002) 2384.
- [4] D.S. Sholl, A. Asthagiri, T.D. Power, *J. Phys. Chem. B* 105 (2001) 4771.
- [5] R.H. Hazen, D.S. Sholl, *Nat. Mater.* 2 (2003) 367.
- [6] T.D. Power, A. Asthagiri, D.S. Sholl, *Langmuir* 18 (2002) 3737.
- [7] P.H. Citrin, P. Eisenberger, R.C. Hewitt, *Phys. Rev. Lett.* 45 (1980) 1948.
- [8] S.B. DiCenzio, G.K. Wertheim, D.N.E. Buchanan, *Appl. Phys. Lett.* 40 (1982) 888.
- [9] S.B. DiCenzio, G.K. Wertheim, D.N.E. Buchanan, *Surf. Sci.* 121 (1982) 411.
- [10] J. Inukai, Y. Osawa, K. Itaya, *J. Phys. Chem. B* 102 (1998) 10034.
- [11] P.A. Dowben, *CRC Crit. Rev. Solid State Mater. Sci.* 13 (1987) 191.
- [12] C.J. Jenks, B.E. Bent, N. Bernstein, F. Zaera, *J. Phys. Chem. B* 104 (2000) 3008.
- [13] C.J. Jenks, B.E. Bent, F. Zaera, *J. Phys. Chem. B* 104 (2000) 3017.
- [14] C.F. McFadden, A.J. Gellman, *Surf. Sci.* 391 (1997) 287.
- [15] G. Kresse, J. Furthmuller, *J. Comp. Mater. Sci.* 6 (1996) 15.
- [16] K. Doll, N.M. Harrison, *Chem. Phys. Lett.* 317 (2000) 282.
- [17] J. Horvath, P. Kamakoti, D.S. Sholl, A.J. Gellman, in preparation.
- [18] A.J. Gellman, J.D. Horvath, M.T. Buelow, *J. Mol. Catal. A* 167 (2001) 3.
- [19] P.J. Feibelman, S. Esch, T. Michely, *Phys. Rev. Lett.* 77 (1996) 2257.
- [20] P.J. Feibelman, *Phys. Rev. B* 49 (1994) 14632.
- [21] A.J. Gellman, J.D. Horvath, M.T. Buelow, *J. Mol. Catal. A* 167 (2001) 3.
- [22] H.C. Jeong, E.D. Williams, *Surf. Sci. Rep.* 34 (1999) 175.
- [23] M. Giesen, G.S. Icking Konert, D. Stapel, H. Ibach, *Surf. Sci.* 366 (1996) 229.
- [24] A. Asthagiri, P.J. Feibelman, D.S. Sholl, *Top. Catal.* 18 (2002) 193.
- [25] S. Dieluwweit, H. Ibach, M. Giesen, T.L. Einstein, *Phys. Rev. B* 67 (2002) 121410.
- [26] X. Zhao, S. Perry, *J. Mol. Catal. A* 216 (2004) 257.
- [27] A.J. Gellman, C.F. McFadden, *Surf. Sci.* 391 (1997) 287.